



NUMERICAL APPROXIMATION WITH THE SPLITTING ALGORITHM TO A SOLUTION OF THE MODIFIED REGULARIZED LONG WAVE EQUATION

Melike KARTA

Department of Mathematics, Ağrı İbrahim Çeçen University, Ağrı, TÜRKİYE

ABSTRACT. In this article, a Lie-Totter splitting algorithm, which is highly reliable, flexible and convenient, is proposed along with the collocation finite element method to approximate solutions of the modified regular long wave equation. For this article, quintic B-spline approximation functions are used in the implementation of collocation methods. Four numerical examples including a single solitary wave, the interaction of two- three solitary waves, and a Maxwellian initial condition are presented to test the closeness of the solutions obtained by the proposed algorithm to the exact solutions. The solutions produced are compared with those in some studies with the same parameters that exist in the literature. The fact that the present algorithm produces results as intended is a proof of how useful, accurate and reliable it is. It can be stated that this fact will be very useful the application of the presented technique for other partial differential equations, with the thought that it may lead the reader to obtain superior results from this study.

1. INTRODUCTION

Nonlinear partial differential equations play an important role in the modeling of many disciplines. The generalized regularized long wave (GRLW), presented in the form below, is among these equations

$$U_t + U_x - \mu U_{xxt} + \epsilon U^p U_x = 0 \quad (1)$$

in which p is positive integer, μ and ϵ non-negative constants. The solutions of this equation, which have an important place in the propagation of nonlinear dispersion waves, are among the solitary wave types, which are packets or pulses propagating in a nonlinear dispersion medium. They have shapes that are not affected by

2020 *Mathematics Subject Classification.* 65N30, 65D07, 33F10, 97N40, 76B25.

Keywords. The modified regularized long wave equation, B-splines, collocation method, Lie-Trotter splitting.

✉ mkarta@agri.edu.tr, 0000-0003-3412-4370.

collisions. These waves preserve their stable wave form since the nonlinear and dispersive effects have dynamical balance. Sometimes it is not easy to obtain analytical solutions of all partial differential equations. In this case, various numerical methods have been developed to obtain approximate solutions to such problems. Some authors have proposed various approaches to solve Eq.(1) numerically. A few of them can be given as Petrov-Galerkin finite element method, Petrov-Galerkin scheme and lumped Galerkin method based on cubic B-splines, respectively, by Refs. [6, 37, 46], and a collocation method with cubic, septic and quintic B-splines, respectively, by Refs. [10, 20, 47], and also Chebyshev-spectral collocation scheme by Ref. [14], parabolic Monge-Ampere moving mesh and uniform by Ref. [2], an approximate quasilinearization approach by Ref. [33], basis of reproducing kernel space by Ref. [27], exponential B-spline collocation scheme by Ref. [28] and element-free kp-Ritz method by Ref. [12]. When $p = 1$ in Eq.(1), it becomes the regularized long wave (RLW) equation used to model a significant number of physical phenomena with weak nonlinearity and dispersion waves containing longitudinal dispersive waves in elastic rods, phonon packets in non-linear crystals, the transverse waves in shallow water, a pressure wave in liquid's gas bubbles, ion-acoustic waves and magnetohydrodynamic wave in plasma. This equation was first introduced by [32] then [5] worked. Many studies can be found in the literature for the approximate solution of the RLW equation. Some of those can be given, Refs. [3, 8, 15, 23] with the finite difference method, Refs. [9, 24, 41] with the Galerkin and Petrov Galerkin methods and Refs. [7, 36, 39, 40, 44, 45] with the collocation algorithm as the finite element method. Additionally, it were worked on methods explicit multistep by Ref. [25] and Haar wavelet by Ref. [30] for RLW equation. In the present studied, the modified regularized long wave equation will be discussed

$$U_t + U_x - \mu U_{xxt} + 6U^2U_x = 0 \tag{2}$$

given with initial condition

$$U(x, 0) = g(x), \quad x_L \leq x \leq x_R \tag{3}$$

and boundary conditions

$$\begin{aligned} U(x_L, t) &= U(x_R, t) = 0, \\ U_x(x_L, t) &= U_x(x_R, t) = 0, \\ U_{xx}(x_L, t) &= U_{xx}(x_R, t) = 0. \end{aligned} \tag{4}$$

It can be seen that the approximate solutions of the MRLW equation have been calculated by many methods in the literature. For example, as the finite element method, while the Galerkin and Petrov Galerkin approaches were studied by Refs. [16, 18, 37], the collocation algorithm with B-splines was studied by Refs. [11, 13, 16, 19, 21, 22, 34, 36], At the same time, [17] used finite difference scheme for the MRLW, [1] solved the equation with mesh free collocation method using radial basis function and [38] acquired the solutions of the equation with the help of Butcher's fifth-order Runge-Kutta (BFRK) scheme.

In this paper, the numerical algorithm of the MRLW equation has been obtained by obtaining two numerical schemes with the help of the Lie-Trotter splitting algorithm and the quintic B-spline collocation method has been applied to each scheme. Thanks to this algorithm, the motion of a single solitary wave, the interaction of two and three solitary waves and the Maxwell initial state have been examined and thus numerical solutions produced with a hybrid approach have been obtained as targeted. Furthermore, Linear stability analysis has been investigated with the help of Von Neumann method.

2. THE SPLITTING ALGORITHM

One of the developed methods to produce numerical solutions of partial differential equations is operator splitting methods. A time-dependent partial differential equation, which usually represents complex physical phenomena such as convection, diffusion, reaction in chemical phenomena, or diffusion, may consist of a combination of one or more operators. Although the computational power of computers has increased rapidly in recent years, good results may not be obtained even if a lot of time is spent in obtaining numerical solutions of a complex problem. Operator splitting methods can be a good approach to numerical solution of such problems. One of these methods is the first-order Lie-Trotter splitting method according to time. This method is the simplest splitting method that reduces the solution of the Cauchy problem given as below to the successive solution of two subproblems

$$\frac{dU(t)}{dt} = \Lambda U(t), \quad U(0) = U_0, t \geq 0, \quad (5)$$

where operator Λ can be written as the sum of operators \hat{A} and \hat{B} . In this case, equation (5) can be written in the following form

$$\frac{dU(t)}{dt} = \hat{A}U(t) + \hat{B}U(t), \quad U(0) = U_0, t \geq 0, \quad (6)$$

in which $U_0 \in X$ is the vector obtained from the initial condition, $u(x, t)$ is solution vector, the operators $\Lambda, \hat{A}, \hat{B}$ are bounded or unbounded operators in a finite or infinite Banach space X . To solve the equation (6) numerically, firstly splitting technique split the equation into as follows

$$\frac{dU(t)}{dt} = \hat{A}U(t), \quad \frac{dU(t)}{dt} = \hat{B}U(t). \quad (7)$$

Here, let $\rho_{\Delta t}^{[\hat{A}]}$ and $\rho_{\Delta t}^{[\hat{B}]}$ be the numerical solutions of the equations containing the expressions \hat{A} and \hat{B} in expression (7), and let the exact solution of (6) be given as $\psi_{\Delta t}$. The simplest splitting methods are introduced as follows

$$\rho_{\Delta t}^{[\hat{B}]} \circ \rho_{\Delta t}^{[\hat{A}]} = e^{\Delta t \hat{B}} e^{\Delta t \hat{A}} \quad \text{or} \quad \rho_{\Delta t}^{[\hat{A}]} \circ \rho_{\Delta t}^{[\hat{B}]} = e^{\Delta t \hat{A}} e^{\Delta t \hat{B}}.$$

and it is known as the Lie-Trotter splitting technique [42] in the literature. Using the Taylor series, It can be stated that the following approximation for an initial

value U_0 is a first-order approximation to the solution of equation (6)

$$\psi_{\Delta t}(U_0) = (\rho_{\Delta t}^{[\hat{A}]} \circ \rho_{\Delta t}^{[\hat{B}]})(U_0) + O(\Delta t^2).$$

Let the formal solution of (6) be given in the form

$$U(t_{n+1}) = e^{\Lambda \Delta t} U(t_n) = e^{(\hat{A} + \hat{B}) \Delta t} U(t_n). \tag{8}$$

Unfolding Taylor series for this solution can be given in the following form

$$U(t_{n+1}) = e^{\Delta t(\hat{A} + \hat{B})} U(t_n) = \sum_{k=0}^{\infty} \frac{t^k}{k!} (\hat{A}(u(t)) \frac{\partial}{\partial U} + \hat{B}(u(t)) \frac{\partial}{\partial U})^k U(t_n).$$

By calculating the sum of the operators \hat{A} and \hat{B} instead of Λ , a new approach to Equation (6) can be obtained, presented in the form below

$$U(t_{n+1}) = e^{\hat{A} \Delta t} e^{\hat{B} \Delta t} U(t_n). \tag{9}$$

An error occurs if (9) is used instead of the equation (8). This is a local splitting error given as follows

$$\begin{aligned} Te &= \frac{1}{\Delta t} (e^{\Delta t(\hat{A} + \hat{B})} - e^{\Delta t \hat{B}} e^{\Delta t \hat{A}}) U(t_n) \\ &= \frac{1}{\Delta t} \left[\frac{\Delta t^2}{2} (\hat{A} \hat{B} - \hat{B} \hat{A}) U(t_n) + O(\Delta t^3) \right] \\ &= \frac{1}{\Delta t} [\hat{A}, \hat{B}] U(t_n) + O(\Delta t^2) \end{aligned}$$

To explain in more detail: Splitting technique splits the given original problem into two parts according to the time. As a result, subproblems with a simpler structure are obtained. Thus, the solution of the original problem is obtained from the solution of the subproblems. In the Lie-Trotter schemes, the first subproblem with operator \hat{A} is solved using the original initial condition given with the problem. Then, the solutions generated with the operator \hat{A} are utilized as the initial condition for the solution of the second sub-problem given with the operator \hat{B} and presented as the solution of the main problem in the first time step. In this way, approximate solutions at the next time levels are obtained similarly to those in the first time step. Algorithm of the mentioned technique with $t_0 = 0$ and $t_N = T$,

$$\begin{aligned} \frac{dU^*(t)}{dt} &= \hat{A}U^*(t), \quad U^*(t_n) = U_n^0, \quad t \in [t_n, t_{n+1}], \\ \frac{dU^{**}(t)}{dt} &= \hat{B}U^{**}(t), \quad U^{**}(t_n) = U^*(t_{n+1}), \quad t \in [t_n, t_{n+1}]. \end{aligned}$$

where U_n^0 is the original initial condition given in (5), Δt is the time step, $\Delta t = t_{n+1} - t_n, n = 0, 1, \dots, N - 1$. Thus, the targeted solutions are obtained with $U(t_{n+1}) = u^{**}(t_{n+1})$. This scheme is called as $(\hat{A} - \hat{B})$ -shaped splitting scheme. It can be stated here that solving the sub-problems separately is more advantageous in terms of computational cost rather than solving the whole problem [26, 43].

3. THE QUINTIC B-SPLINES

In order to make approximate calculations of the MRLW equation, the solution region is limited to the interval $x_R \leq x \leq x_N$. This range is partitioned by nodes x_j into uniformly finite elements of length h such that $x_L = x_0 \leq x_1 \leq \dots \leq x_N = x_R$ and $h = x_{j+1} - x_j$. The set of quintic B-splines $\varphi_j(x)$ for $j = -2(1)N + 2$ forming a base on the interval $[x_L, x_R]$ at nodes x_j is presented as follows by [31]

$$\varphi_j(x) = \frac{1}{h^5} \begin{cases} p_0 = (x - x_{j-3})^5, & x \in [x_{j-3}, x_{j-2}] \\ p_1 = p_0 - 6(x - x_{j-2})^5, & x \in [x_{j-2}, x_{j-1}] \\ p_2 = p_1 - 6(x - x_{j-2})^5 + 15(x - x_{j-1})^5, & x \in [x_{j-1}, x_j] \\ p_3 = p_2 - 6(x - x_{j-2})^5 - 20(x - x_j)^5, & x \in [x_j, x_{j+1}] \\ p_4 = p_3 - 6(x - x_{j-2})^5 + 15(x - x_{j+1})^5, & x \in [x_{j+1}, x_{j+2}] \\ p_5 = p_4 - 6(x - x_{j-2})^5 - 6(x - x_{j+2})^5, & x \in [x_{j+2}, x_{m,j3}] \\ 0, & \text{otherwise.} \end{cases} \quad (10)$$

The numerical solution $U_N(x, t)$ corresponding to the exact solution $U(x, t)$ is searched in terms of quintic B-splines in the following form

$$U_N(x, t) = \sum_{j=-2}^{N+2} \varphi_j(x) \delta_j(t) \quad (11)$$

Here, $\delta_j(t)$ are the unknown time parameters determined with both boundary and collocation conditions. When the trial function (10) is substituted in the equation (11), The knot values U_j, U'_j, U''_j at nodes x_j are acquired in terms of the parameter $\delta_j(t)$ with form

$$\begin{aligned} U_j &= \delta_{m-2} + 26\delta_{j-1} + 66\delta_j + 26\delta_{j+1} + \delta_{j+2}, \\ U'_j &= \frac{5}{h}(-\delta_{j-2} - 10\delta_{j-1} + 10\delta_{j+1} + \delta_{j+2}), \\ U''_j &= \frac{20}{h^2}(\delta_{j-2} + 2\delta_{j-1} - 6\delta_j + 2\delta_{j+1} + \delta_{j+2}), \end{aligned} \quad (12)$$

Here, the first and second derivatives with respect to x are denoted by the symbols ' and ". The all of quintic B-spline base functions are zero outside of $\phi_{j-2}, \phi_{j-1}, \phi_j, \phi_{j+1}, \phi_{j+2}$ and ϕ_{j+3} .

4. THE IMPLEMENTATION OF COLLOCATION METHOD

In this section, firstly, the MRLW equation with the initial-boundary value problem is split. In an other saying, the main problem is divided into sub-equations as follows to obtain two partial differential equations, one linear and the other nonlinear, with respect to time

$$U_t - \mu U_{xxt} + U_x = 0 \quad (13)$$

$$U_t - \mu U_{xxt} + 6U^2 U_x = 0. \tag{14}$$

When U_j and its first derivatives U'_j and U''_j given in the (12) equation are substituted in equations (13) and (14), system of ordinary differential equations given in the following form are obtained for $j = 0(1)N$ in the entire solution region

$$\begin{aligned} & \dot{\delta}_{m-2} + 26\dot{\delta}_{m-1} + 66\dot{\delta}_m + 26\dot{\delta}_{m+1} + \dot{\delta}_{m+2} \\ & - \mu \frac{20}{h^2} (\delta_{m-2} + 2\delta_{m-1} - 6\delta_m + 2\delta_{m+1} + \delta_{m+2}) \\ & + \frac{5}{h} (-\delta_{m-2} - 10\delta_{m-1} + 10\delta_{m+1} + \delta_{m+2}) = 0, \end{aligned} \tag{15}$$

$$\begin{aligned} & \dot{\delta}_{m-2} + 26\dot{\delta}_{m-1} + 66\dot{\delta}_m + 26\dot{\delta}_{m+1} + \dot{\delta}_{m+2} \\ & - \mu \frac{20}{h^2} (\delta_{m-2} + 2\delta_{m-1} - 6\delta_m + 2\delta_{m+1} + \delta_{m+2}) \\ & + \frac{5z_j}{h} (-\delta_{m-2} - 10\delta_{m-1} + 10\delta_{m+1} + \delta_{m+2}) = 0 \end{aligned} \tag{16}$$

in which the first derivative according to time t is shown with symbol "." and z_j is gotten as

$$z_j = 6(\delta_{j-2} + 26\delta_{j-1} + 66\delta_j + 26\delta_{j+1} + \delta_{j+2})^2$$

to linearize the (16) system. Then, by applying $\frac{\delta_j^{n+1} + \delta_j^n}{2}$ for spatial discretization and $\frac{\delta_j^{n+1} - \delta_j^n}{\Delta t}$ for time discretization to these two systems, two numerical schemes are obtained with form

$$\begin{aligned} & k_1\delta_{m-2}^{n+1} + k_2\delta_{m-1}^{n+1} + k_3\delta_m^{n+1} + k_4\delta_{m+1}^{n+1} + k_5\delta_{m+2}^{n+1} \\ & = k_6\delta_{m-2}^n + k_7\delta_{m-1}^n + k_8\delta_m^n + k_9\delta_{m+1}^n + k_{10}\delta_{m+2}^n, \end{aligned} \tag{17}$$

$$\begin{aligned} & l_1\delta_{m-2}^{n+1} + l_2\delta_{m-1}^{n+1} + l_3\delta_m^{n+1} + l_4\delta_{m+1}^{n+1} + l_5\delta_{m+2}^{n+1} \\ & = l_6\delta_{m-2}^n + l_7\delta_{m-1}^n + l_8\delta_m^n + l_9\delta_{m+1}^n + l_{10}\delta_{m+2}^n \end{aligned} \tag{18}$$

in which $k_i, l_i (i = 1(1)10)$ and z_j are $z_j = 6U^2$

$$\begin{aligned} k_1 &= 1 - \frac{20\mu}{h^2} - \frac{5\Delta t}{2h}, k_2 = 26 - \frac{40\mu}{h^2} - \frac{25\Delta t}{h}, k_3 = 66 + \frac{120\mu}{h^2}, \\ k_4 &= 26 - \frac{40\mu}{h^2} + \frac{25\Delta t}{h}, k_5 = 1 - \frac{20\mu}{h^2} + \frac{5\Delta t}{h} \end{aligned}$$

$$\begin{aligned} k_6 &= 1 - \frac{20\mu}{h^2} + \frac{5\Delta t}{2h}, k_7 = 26 - \frac{40\mu}{h^2} - \frac{25\Delta t}{h}, k_8 = 66 + \frac{120\mu}{h^2}, \\ k_9 &= 26 - \frac{40\mu}{h^2} + \frac{25\Delta t}{h}, k_{10} = 1 - \frac{20\mu}{h^2} - \frac{5\Delta t}{h} \end{aligned}$$

$$l_1 = 1 - \frac{20\mu}{h^2} - \frac{5z_j\Delta t}{2h}, l_2 = 26 - \frac{40\mu}{h^2} - \frac{25z_j\Delta t}{h}, l_3 = 66 + \frac{120\mu}{h^2},$$

$$l_4 = 26 - \frac{40\mu}{h^2} + \frac{25z_j\Delta t}{h}, l_5 = 1 - \frac{20\mu}{h^2} + \frac{5z_j\Delta t}{2h}.$$

$$l_6 = 1 - \frac{20\mu}{h^2} + \frac{5z_j\Delta t}{2h}, l_7 = 26 - \frac{40\mu}{h^2} + \frac{25z_j\Delta t}{h}, l_8 = 66 + \frac{120\mu}{h^2},$$

$$l_9 = 26 - \frac{40\mu}{h^2} - \frac{25z_j\Delta t}{h}, l_{10} = 1 - \frac{20\mu}{h^2} - \frac{5z_j\Delta t}{2h}.$$

(17) and (18) are systems consisting of $(N + 1)$ equations with $(N + 5)$ unknowns. These systems contain four additional element parameters $\delta_{-2}, \delta_{-1}, \delta_{N+1}, \delta_{N+2}$ outside the solution region of the problem. To obtain the only solution of systems (17) and (18), the parameters that are not in the solution region must be eliminated from these systems. For this purpose, the nodal values of U_j and $(U_j)'$ in the equation (12) and the boundary conditions $U(x_L, t) = U(x_R, t) = 0$ and $U_x(x_L, t) = U_x(x_R, t) = 0$ are used. Thus, systems (17) and (18) are reduced to the $(N + 1) \times (N + 1)$ matrix system.

For approximate solutions of the (17) and (18) systems, it is necessary to find the initial vector δ_j^0 . This required initial vector is found by solving the system of algebraic equations given in the following form, using the initial condition $U(x_j, 0) = U_N(x_j, 0) = g_0(x_j)$, and the approach $U_N(x, 0) = \sum_{j=-2}^{N+2} \varphi_j(x)\delta_j^0(0)$

$$\begin{aligned} U_m &= \delta_{j-2}^0 + 26\delta_{j-1}^0 + 66\delta_j^0 + 26\delta_{j+1}^0 + \delta_{j+2}^0, j = 0(1)N, \\ U_0 &= \delta_{-2}^0 + 26\delta_{-1}^0 + 66\delta_0^0 + 26\delta_1^0 + \delta_2^0, \\ U_1 &= \delta_{-1}^0 + 26\delta_0^0 + 66\delta_1^0 + 26\delta_2^0 + \delta_3^0, \\ &\cdot \\ &\cdot \\ &\cdot \\ U_{N-1} &= \delta_{N-3}^0 + 26\delta_{N-2}^0 + 66\delta_{N-1}^0 + 26\delta_N^0 + \delta_{N+1}^0, \\ U_N &= \delta_{N-2}^0 + 26\delta_{N-1}^0 + 66\delta_N^0 + 26\delta_{N+1}^0 + \delta_{N+2}^0. \end{aligned} \tag{19}$$

with unknown element parameters δ_j^0 . By using the boundary conditions $U_x(x_L, t) = U_x(x_R, t) = 0$ and $U_{xx}(x_L, t) = U_{xx}(x_R, t) = 0$ for these systems, $\delta_{-2}, \delta_{-1}, \delta_{N+1}, \delta_{N+2}$ are eliminated so that the following matrix equation is obtained

$$\lambda b^0 = d$$

schemes for linear or linearized partial differential equations. Via the Euler formula $e^{i\Phi} = \cos\Phi + i\sin\Phi$, growth factors ϱ_1 and ϱ_2 submitted as follows are acquired

$$\varrho_1 = \frac{A_1 - iB_1}{A_1 + iB_1}, \quad \varrho_2 = \frac{A_1 - iC_1}{A_1 + iC_1}, \quad (22)$$

$$A_1 = \left(2 - \frac{40\mu}{h^2}\right)\cos(2\gamma h) + \left(52 - \frac{80\mu}{h^2}\right)\cos(\gamma h) + \left(66 + \frac{120\mu}{h^2}\right),$$

$$B = \frac{5\Delta t}{h}\sin(2\gamma h) + \frac{50\Delta t}{h}\sin(\gamma h),$$

and

$$C = \frac{5z_m\Delta t}{h}\sin(2\gamma h) + \frac{50z_m\Delta t}{h}\sin(\gamma h).$$

For $k_1, k_2, \dots, k_9, k_{10}$ and $l_1, l_2, \dots, l_9, l_{10}$ founded in section 3. $|\varrho_1| = |\varrho_2| = 1$ from Equation (22) and hence, for the whole system with Lie Trotter-Splitting algorithm can be written as $|\varrho_1| \cdot |\varrho_2| = 1$. Because the conditions $|\varrho_1| \leq 1$, and $|\varrho_2| \leq 1$ according to the von Neumann theory are satisfied, it can be clearly said that the systems (17) and (18) are unconditionally stable.

6. NUMERICAL EXPERIMENTS AND DISCUSSION

For numerical calculations of main problem are considered to the movement of single solitary wave, two and three solitary wave interactions and the Maxwellian initial condition. The difference between the exact and approximate solutions is calculated by choosing some specific times to match the studies in the literature. For this, the following error norms are used

$$L_2 = \|U - U_N\|_2 = \sqrt{h \sum_{j=0}^N (U - U_N)^2},$$

and

$$L_\infty = \|U - U_N\|_\infty = \max_j |U - U_N|.$$

To check the conservation of numerical schemes during the simulation of solitary wave motion, the invariants I_1, I_2 and I_3 are calculated, which correspond to the conservation of mass, momentum and energy proved by Olver [29] and presented as follows

$$I_1 = \int_{x_L}^{x_R} U(x, t) dx,$$

$$I_2 = \int_{x_L}^{x_R} [U^2(x, t) + \mu U_x^2(x, t)] dx,$$

$$I_3 = \int_{x_L}^{x_R} [U^4(x, t) - \mu U_x^2(x, t)] dx.$$

6.1. **Example I: The movement of a single solitary wave.** This example considers the MRLW equation by taking into accounting boundary condition $U \rightarrow 0$ when $x \rightarrow \pm\infty$ and initial condition

$$U(x, 0) = \sqrt{c} \operatorname{sech}[s(x - x_0)].$$

The exact solution for this problem is presented in the following form

$$U(x, t) = \sqrt{c} \operatorname{sech}[s(x - (c + 1)t - x_0)].$$

Here, c and x_0 are arbitrary constants and $s = \sqrt{\frac{c}{\mu(c+1)}}$. The exact values of the conservation quantities of a single solitary wave with width s and amplitude \sqrt{c} as in [11] are given as follows

$$\begin{aligned} I_1 &= \int_{x_L}^{x_R} U(x, t) dx = \frac{\pi\sqrt{c}}{s}, \\ I_2 &= \int_{x_L}^{x_R} [U^2(x, t) + \mu U_x^2(x, t)] dx = \frac{2c}{s} + \frac{2\mu sc}{3}, \\ I_3 &= \int_{x_L}^{x_R} [U^4(x, t) - \mu U_x^2(x, t)] dx = \frac{4c^2}{3s} - \frac{2\mu sc}{3}. \end{aligned} \tag{23}$$

For solitary wave motion with amplitude 1, All of calculations and comparisons in Table 1-2 are done with $\mu = 1, x_0 = 40, c = 1, \Delta t = 0.025$ and $h = 0.2$ over $[0, 100]$ to match those in [11, 16, 21, 22, 36, 37]. Table 1 reports the invariant and error norm amounts of the current approach from $t = 0$ to 10 with one increment value. This table shows that the calculated invariants are compatible with each other and gratifying because the error norms L_2 and L_∞ are quite small. Furthermore, it can be seen from Table 1 that the the changing of invariants I_1, I_2, I_3 are less than $0.8 \times 10^{-7}, 1.1 \times 10^{-7}, 1.26 \times 10^{-5}$, respectively. The comparison of the ones of the previously recorded methods with the results of the proposed technique is given in Table 2 at time $t = 10$. Looking at the table, it can be easily seen that the current approach produces the best results for error norms and the computed invariant values are in agreement with the analytical ones $I_1 = 4.4428829, I_2 = 3.2998316$ and $I_3 = 1.4142135$. The motion of a single solitary wave at various time levels with parameters $\Delta t = 0.025, h = 0.2, c = 1$ is plotted in Fig.1 and this figure shows that the soliton shifts to the right at a constant velocity with an almost unchanged amplitude even as time increases, as hoped. At $t = 0$, the amplitude is 1 which is situated at $x = 40$ and $x = 60$.

For Table 3-4, the parameters $\mu = 1, x_0 = 40, c = 0.3, \Delta t = 0.01$ and $h = 0.1$ over $[0, 100]$ are selected as in n Refs. [21]. Thus, The amplitude of the solitary wave is 0.547723. Table 3 displays the invariant and error norm amounts of the present approach from $t = 0$ to 20 with two increment value. From this table, it can be observed that very small and pleasing solutions are obtained with the Lie-Trotter splitting technique. Invariants I_1, I_3 are compatible with each other and I_2 remains constant. Furthermore, it can be seen from Table 3 that the the

TABLE 1. The error norms and invariants of the single solitary wave with $\Delta t = 0.025, h = 0.2$, for $c = 1$ on the region $[0, 100]$

t	I_1	I_2	I_3	$L_2 \times 10^3$	$L_\infty \times 10^3$
0	4.44288294	3.29983161	1.41421360	0.00000000	0.00000000
1	4.44288293	3.29983161	1.41420559	1.56533150	1.02551887
2	4.44288292	3.29983159	1.41419884	2.41711399	1.40020924
3	4.44288292	3.29983158	1.41419842	2.67081261	1.22652109
4	4.44288291	3.29983157	1.41419926	2.68157587	1.04668636
5	4.44288290	3.29983156	1.41419995	2.62782252	1.10627938
6	4.44288289	3.29983155	1.41420040	2.56931532	1.11288942
7	4.44288289	3.29983153	1.41420067	2.52306335	1.07889684
8	4.44288288	3.29983152	1.41420084	2.49240521	1.02360259
9	4.44288287	3.29983151	1.41420094	2.47654106	0.95806880
10	4.44288286	3.29983150	1.41420100	2.47366508	0.89643465

TABLE 2. Comparisons of the error norms and invariants of the single solitary wave with $\Delta t = 0.025, h = 0.2$, for $c = 1$ on the region $[0, 100]$ at $t = 10$

method	I_1	I_2	I_3	$L_2 \times 10^3$	$L_\infty \times 10^3$
Exact	4.4428829	3.2998316	1.4142135	0	0
Present	4.4428829	3.2998315	1.4142010	2.47366508	0.89643465
[21]	4.4428661	3.2997108	1.4143165	2.58891	1.35164
[22]	4.44288	3.29983	1.41420	9.30196	5.43718
[16]	4.4431919	3.3003022	1.4146930	2.41750	1.08099
[36]	4.445176	3.302476	1.417411	0.8644	1.2475
[11]1	4.442	9.299	1.413	19.39	9.24
[11]2	4.440	3.296	1.411	20.3	11.2
[37]	4.44288	3.29981	1.41416	3.00533	1.68749

changing of invariants I_1, I_3 are less than 1.4×10^{-7} , 0.9×10^{-7} , respectively and 0 of I_2 during the execution of the program. Table 4 presents a comparison of the results of the proposed study and other registered ones by calculating error norms L_2 and L_∞ and invariant values I_1, I_2 and I_3 . All comparisons are made for time $t=20$. As a result of this comparison, it can easily be seen that the present technique produces more satisfactory results. Invariant values are consistent with those compared. The motion of a single solitary wave at various time levels with parameters $\Delta t = 0.01, h = 0.1, c = 0.3$ is plotted in Fig.2. Fig.3 shows the graphs of the error distributions of the solitary wave with amplitude of 1 and 0.3 respectively, at $t = 10$ and 20.

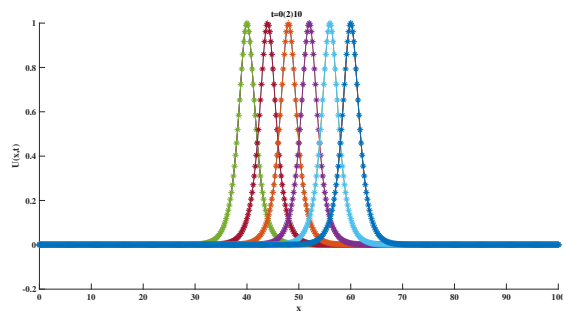


FIGURE 1. Movement of a single solitary wave at $t = 0(2)10$ for MRLW equation

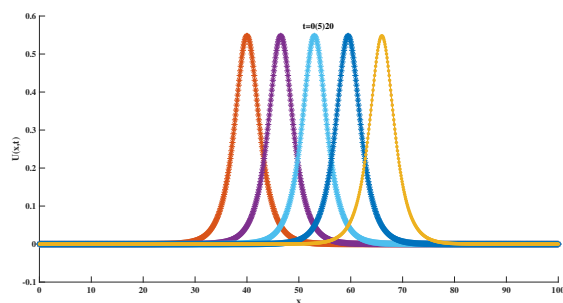


FIGURE 2. Movement of a single solitary wave at $t = 0(5)20$ for MRLW equation

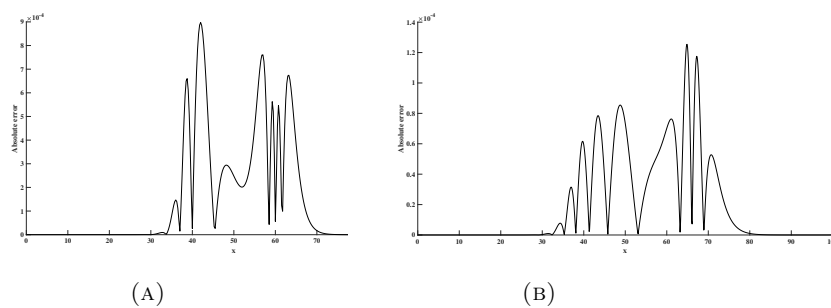


FIGURE 3. Error distribution graphs for a) $\Delta t = 0.025, h = 0.2, c = 1$ and b) $\Delta t = 0.01, h = 0.1, c = 0.3$ over $[0, 100]$.

TABLE 3. The error norms and invariants of the single solitary wave with $\Delta t = 0.01$, $h = 0.1$, for $c = 0.3$ on the region $[0, 100]$

t	I_1	I_2	I_3	$L_2 \times 10^3$	$L_\infty \times 10^3$
0	3.58196673	1.34507649	0.15372303	0.00000000	0.00000000
2	3.58196674	1.34507649	0.15372299	0.17472238	0.09673881
4	3.58196675	1.34507649	0.15372294	0.28047087	0.14367750
6	3.58196676	1.34507649	0.15372293	0.32725879	0.14066701
8	3.58196677	1.34507649	0.15372293	0.34590142	0.13215052
10	3.58196678	1.34507649	0.15372293	0.35279733	0.13158877
12	3.58196678	1.34507649	0.15372294	0.35465095	0.13057054
14	3.58196679	1.34507649	0.15372294	0.35426140	0.12926338
16	3.58196678	1.34507649	0.15372294	0.35288262	0.12791317
18	3.58196674	1.34507649	0.15372294	0.35110940	0.12661543
20	3.58196659	1.34507649	0.15372294	0.34923321	0.12540476

TABLE 4. Comparisons of the error norms and invariants of the single solitary wave with $\Delta t = 0.01$, $h = 0.1$, for $c = 0.3$ on the region $[0, 100]$ at $t = 20$

method	I_1	I_2	I_3	$L_2 \times 10^4$	$L_\infty \times 10^4$
Present	3.58196659	1.34507649	0.15372294	0.34923321	0.12540476
[21]	3.5820204	1.3450974	0.1537250	0.8112594	0.3569076
[22]	3.58197	1.34508	0.153723	6.06885	2.96650
[16]	3.5820206	1.3450944	0.1537284	1.2273638	0.4472294
[36]	3.582265	1.345182	0.1538901	3.379583	7.672911
[1]MQ	3.5819665	1.3450764	0.153723	0.51498	0.22551
[1]TPS	3.5819663	1.3450759	0.153723	0.51498	0.26605
[13]	3.581967	1.345076	0.153723	0.5089274	0.2222848

6.2. Example II: Interaction of two solitary waves. This example considers the problem of interaction of two solitary waves with various amplitudes and for Eq.(2), the following initial conditions are written as the linear sum of two well-separated solitary waves with different amplitudes

$$U(x, 0) = \sum_{i=1}^2 a_i \operatorname{sech}[s_i(x - x_i)],$$

in which c_i and x_i are arbitrary constants, $a_i = \sqrt{c_i}$, $s_i = \sqrt{\frac{c_i}{\mu(c_i+1)}}$, $i = 1(1)2$. The exact values of the conservation quantities are given as follows [11]

$$I_1 = \sum_{i=1}^2 \frac{\pi\sqrt{c_i}}{s_i},$$

$$I_2 = \sum_{i=1}^2 \frac{2c_i}{s_i} + \frac{2\mu s_i c_i}{3},$$

$$I_3 = \sum_{i=1}^2 \frac{4c_i^2}{3s_i} - \frac{2\mu s_i c_i}{3}.$$

Numerical simulation is done on the $[0, 250]$ region by selecting the parameters $\mu = 1, x_1 = 25, x_2 = 55, c_1 = 4, c_2 = 1, \Delta t = 0.025, h = 0.2$ as in Ref. [21]. The experimental results obtained by running the numerical experiments at $t=0(2)20$ times are shown in Table 5. The exact values of the invariants are $I_1 = 11.467698, I_2 = 14.629243$ and $I_3 = 22.880466$. Table 5 submits a comparison of the solutions in the proposed method with those in the references [1, 16, 19, 21, 22, 34, 37, 38] and this table displays that the invariant quantities I_1, I_2 and I_3 are quite conservative and the values found are consistent with their exact values throughout the operation of the computer program. Fig.4 reports the interactions of two solitary waves at various time levels. It can be clearly seen from this figure that at $t = 0$, the wave with the smaller amplitude is to the right of the wave with the larger amplitude. Since the shorter wave moves slower than the longer one, the longer wave catches the short wave at $t = 12$ and collides. Later, it fars away from the shorter one with the advancing time. At $t = 20$, while the amplitude of the smaller wave becomes 1.014 at $x = 84.2$ the amplitude of the larger wave becomes 1.998 at $x = 97.4$.

6.3. Example III:Interaction of three solitary waves. This example deals with the problem of interaction of three solitary waves with different amplitudes and advancing in the same direction and for MRLW equation, the following initial conditions are written as the linear sum of three well-separated solitary waves with different amplitudes

$$U(x, 0) = \sum_{i=1}^3 a_i \operatorname{sech}[s_i(x - x_i)],$$

in which c_i and x_i are arbitrary constants, $a_i = \sqrt{c_i}$, $s_i = \sqrt{\frac{c_i}{\mu(c_i+1)}}$, $i = 1(1)3$. The exact values of the conservation quantities obtained from Eq.(18) are given as follows

$$I_1 = \sum_{i=1}^3 \frac{\pi\sqrt{c_i}}{s_i},$$

TABLE 5. Comparison of invariants of two solitary waves with values $\Delta t = 0.025, h = 0.2$, for $x_1 = 25, x_2 = 55, c_1 = 4, c_2 = 1$ on the region $[0, 250]$ at $t = 0(2)20$ with those in [13]

t	method			[13]		
	I_1	I_2	I_3	I_1	I_2	I_3
0	11.46769804	14.62924273	22.88046615	11.467698	14.629277	22.880432
2	11.46769804	14.62924273	22.88046615	11.467698	14.624259	22.860365
4	11.46769804	14.62924273	22.88046615	11.467698	14.619226	22.840279
6	11.46769804	14.62924273	22.88046615	11.467699	14.614169	22.820069
8	11.46769804	14.62924273	22.88046615	11.467700	14.606821	22.787857
10	11.46769804	14.62924273	22.88046615	11.467700	14.603687	22.771773
12	11.46788404	14.62924273	22.88046615	11.467699	14.603056	22.775766
14	11.46769804	14.62924273	22.88046615	11.467699	14.598059	22.756029
16	11.46769804	14.62924273	22.88046615	11.467700	14.593048	22.736127
18	11.46769804	14.62924273	22.88046615	11.467700	14.588061	22.716289
20	11.46769804	14.62924273	22.88046615	11.467701	14.583089	22.696510
20 [19]1	11.4676541	14.6292088	22.8803901			
20 [19]2	11.4676452	14.6309639	22.8786025			
20 [34]	11.4677	14.6299	22.8806			
20 [38]	11.4676977	14.62927316	22.8804154			
20 [21]	11.4691886	14.6331334	22.8764330			
20 [16]	11.4662207	14.6253125	22.8650456			
20 [37]	11.4677	14.6299	22.8806			
20 [22]	11.4677	14.6292	22.8809			
20 [1]MQ	11.467698	14.583052	22.696539			
20 [1]TPS	11.467742	14.582424	22.694269			

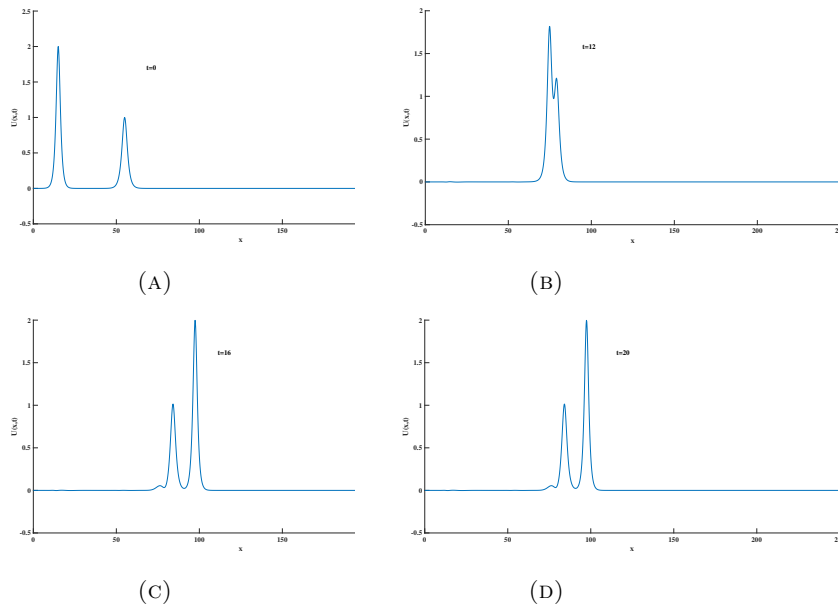


FIGURE 4. The interactions of two solitary waves at various time levels of MRLW equation

$$I_2 = \sum_{i=1}^3 \frac{2c_i}{s_i} + \frac{2\mu s_i c_i}{3},$$

$$I_3 = \sum_{i=1}^3 \frac{4c_i^2}{3s_i} - \frac{2\mu s_i c_i}{3}.$$

During the numerical simulation, the calculation process is performed by taking the parameters $\mu = 1, x_1 = 15, x_2 = 45, x_3 = 60, c_1 = 4, c_2 = 1, c_3 = 0.25, \Delta t = 0.025, h = 0.2$ on the region $[0, 250]$. This process is carried out at times $0(5)45$ and the exact values of the invariants here are $I_1 = 14.9801, I_2 = 15.8218$ and $I_3 = 22.9923$. Table 6 presents a comparison of the solutions in the suggested method with those in the references [1, 21, 22, 34] and this table displays that the invariant quantities I_1, I_2 and I_3 are quite conservative and the values found are consistent with their exact values throughout the operation of the computer program. Here, the interaction of solitary waves using various times is shown in Fig.5. This figure indicates that the interaction started at approximately $t = 10$. there were overlaps at time $t = 40$, and then the waves returned to their original state at $t = 40$.

TABLE 6. Comparison of invariants of three solitary waves with values $\Delta t = 0.025, h = 0.2$, for $x_1 = 15, x_2 = 45, x_3 = 60, c_1 = 4, c_2 = 1, c_3 = 0.25$ on the region $[0, 250]$ at $t = 0(5)45$ with those in [13]

t	method			[13]		
	I_1	I_2	I_3	I_1	I_2	I_3
0	14.97251076	15.82181232	22.99226955	14.980099	15.837528	23.008136
5	14.97251076	15.82181232	22.99226955	14.980105	15.837528	22.957891
10	14.97251076	15.82181232	22.99226955	14.980109	15.807025	22.877972
15	14.97251076	15.82181232	22.99226955	14.980106	15.807032	22.885947
20	14.97251076	15.82181232	22.99226955	14.980106	15.795022	22.837454
25	14.97251076	15.82181232	22.99226955	14.980107	15.782840	22.788852
30	14.97251076	15.82181232	22.99226955	14.980107	15.770634	22.740419
35	14.97251076	15.82181232	22.99226955	14.980108	15.758480	22.692279
40	14.97251076	15.82181232	22.99226955	14.980108	15.746389	22.644448
45	14.97251076	15.82181232	22.99226955	14.968030	15.734374	22.596591
20 [34]	14.930390	15.822500	22.964190			
20 [21]	14.7145273	15.4927592	23.3529062			
20 [22]	13.7043	15.6563	22.9303			
20 [1]MQ	14.96814	15.73434	22.596625			
20 [1]TPS	14.96824	15.73376	22.594494			

6.4. **Example IV: The Maxwellian initial condition.** This last example examines the improvement of the following the Maxwell initial condition in the sequence of solitary waves

$$U(x, 0) = \exp(-(x - 40)^2).$$

Here, the solution behavior for the Maxwellian condition presented above is evaluated with the values of μ . Approximate values of invariants are shown in Table 7. All figures are depicted in Fig. 6 at time 14.5. At the end of the study for values

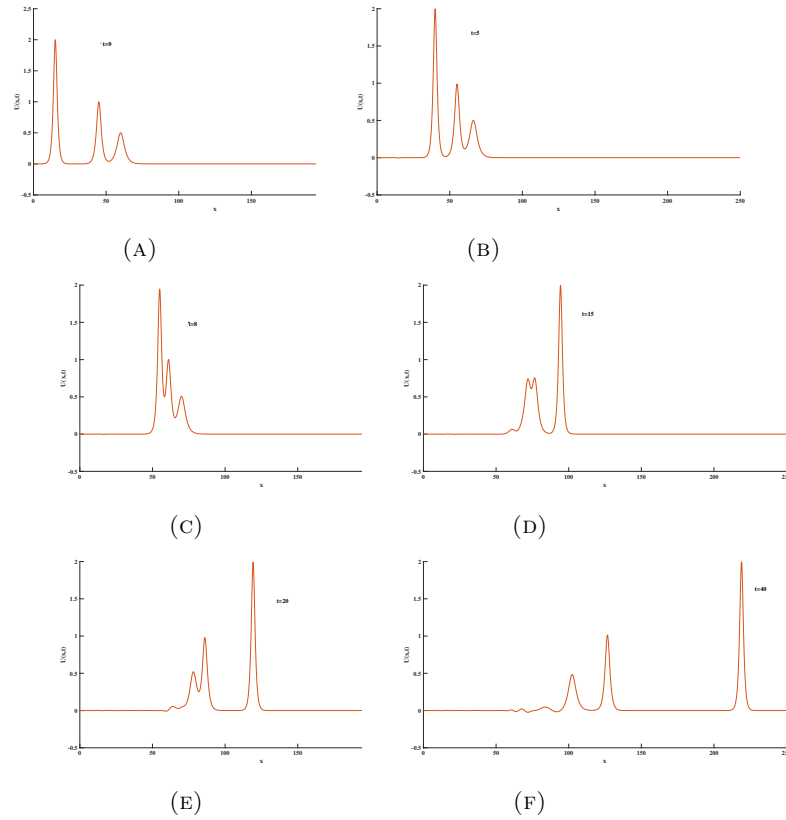


FIGURE 5. The interactions of three solitary waves at various time levels of MRLW equation

$\mu = 0.1, 0.04, 0.015$ and $\mu = 0.01$, it is observed that only a single soliton movement is followed for $\mu = 0.1$ and this is pictured with a). When $\mu = 0.04, 0.015$ are taken, it is shown with b) and c) that two and three stable solitons are occurred and when the value $\mu = 0.01$ is selected, the Maxwellian initial condition decomposes into four solitary waves and it is plotted with d). In all the figures in this example, the presence of a small oscillating tail formed behind the last wave is observed. The peaks of the well-developed wave whose speeds are linearly dependent on their amplitudes lie on a straight line.

7. CONCLUSION

In this article, Lie-trotter splitting algorithm with collocation finite element method has been presented. Four experimental examples are given to measure

TABLE 7. Values of the invariants of the MRLW equation for the Maxwellian initial condition

t	μ	I_1	I_2	I_3	μ	I_1	I_2	I_3
0	0.1	1.77245385	1.37864519	0.76089588	0.015	1.77245385	1.27211379	0.86742727
3		1.77242409	1.37853754	0.66726850		1.74470267	1.23369811	0.72548127
6		1.77237678	1.37846448	0.66768464		1.71890317	1.17440856	0.73866510
9		1.77232940	1.37839090	0.66787415		1.70124953	1.13869004	0.74633211
12		1.77228192	1.37831554	0.66798301		1.68830339	1.11560302	0.75073526
15		1.77223441	1.37823955	0.66805774		1.68128767	1.11897777	0.74641698
0	0.01	1.77245385	1.26584724	0.87369382	0.04	1.77245385	1.30344656	0.83609451
3		1.71307229	1.14513104	0.76148916		1.77091565	1.30148045	0.69106562
6		1.68854075	1.12482375	0.75995674		1.76851865	1.29612046	0.69320291
9		1.66818971	1.08010404	0.76885908		1.76632858	1.29227683	0.69439710
12		1.65804755	1.07686486	0.76703741		1.76426994	1.28925313	0.69497936
15		1.64143143	1.02666184	0.77926968		1.76221840	1.28586712	0.69570702

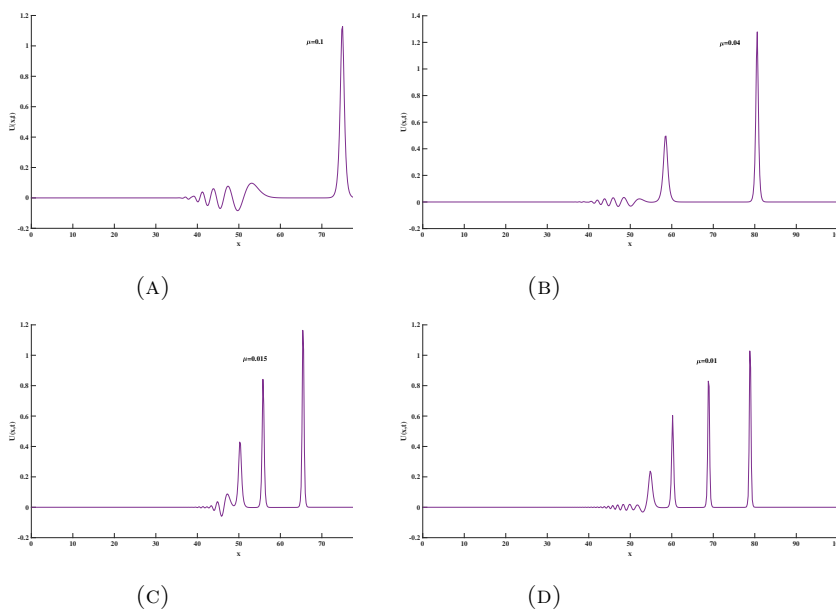


FIGURE 6. The interactions of two solitary waves at various time levels of MRLW equation

the reliability and performance of the method in this study. The error norms L_2 and L_∞ are calculated to show that results are superior to those of the methods in the literature and the results produced have been compared in tables and figures. The error norms are, as hoped, smaller than the results in the literature and thus closer to the analytic solution. The invariants I_1, I_2 and I_3 are satisfactorily well preserved throughout the entire computer run. The computed solutions displays it

can be easily said that the current algorithm will be beneficial in applying to other nonlinear equation types such as MRLW.

Declaration of Competing Interests The author declares that there is no competing interest regarding the publication of this paper.

REFERENCES

- [1] Ali, A., Mesh Free Collocation Method for Numerical Solution of Initial-Boundary Value Problems Using Radial Basis Functions, Dissertation, Ghulam Ishaq Khan Institute of Engineering Sciences and Technology, 2009.
- [2] Alharbi, A.R., Al-Munawarah, A.M., Arabia, S., Numerical investigation for the GRLW equation using parabolic Monge Ampere equation, *Comput. Sci.*, 15 (2020), 443–462.
- [3] Bhardwaj, D., Shankar, R., A computational method for regularized long wave equation, *Comput. Math. Appl.*, 40 (2000), 1397-1404. [https://doi.org/10.1016/S0898-1221\(00\)00248-0](https://doi.org/10.1016/S0898-1221(00)00248-0)
- [4] Başhan, A., Yağmurlu, N.M., A mixed method approach to the solitary wave, undular bore and boundary-forced solutions of the regularized long wave equation, *Comp. Appl. Math.*, 41(169) (2022). <https://doi.org/10.1007/s40314-022-01882-7>
- [5] Benjamin, T.B., Bona, J.L., Mahony, J.J., Model equations for long waves in nonlinear dispersive systems, *Philos. Trans. R. Soc. A Math. Phys. Eng. Sci.*, 272 (1972), 47–78. <https://doi.org/10.1098/rsta.1972.0032>
- [6] Bhowmik, S.K., Karakoc, S.B.G., Numerical approximation of the generalized regularized long wave equation using Petrov–Galerkin finite element method, *Numer. Methods Partial Differ. Equ.*, 35 (2019) 2236–2257. <https://doi.org/10.1002/num.22410>
- [7] Dağ, I., Saka, B., Irk, D., Application of cubic B-splines for numerical solution of the RLW equation, *Appl. Math. Comput.*, 159 (2004) 373–389. <https://doi.org/10.1016/j.amc.2003.10.020>
- [8] Danaf, T.S., Raslan, K.R., Ali, K.K., New numerical treatment for the generalized regularized long wave equation based on finite difference scheme, *Int. J. Soft Comput. Eng.*, 4(2014), 16–24.
- [9] Esen, A., Kutluay, S., Application of a lumped Galerkin method to the regularized long wave equation, *Appl. Math. Comput.*, 174 (2006), 833–845. <https://doi.org/10.1016/j.amc.2005.05.032>
- [10] El-Danaf, T.S., Raslan, K.R., Ali, K.K., Collocation method with cubic B-Splines for solving the GRLW equation, *Int. J. Numer. Methods Appl.*, 15(1) (2016), 39-59. <http://dx.doi.org/10.17654/NM015010039>
- [11] Gardner, L.R.T., Gardner, G.A., Ayoub F.A., Amein, N.K., Approximations of solitary waves of the MRLW equation by B-spline finite element, *Arab. J. Sci. Eng.*, 22 (1997), 183–193.
- [12] Guo, P.F., Zhang, L.W., Liew, K.M., Numerical analysis of generalized regularized long wave equation using the element free kp-Ritz method, *Appl. Math. Comput.*, 240 (2014) 91–101. <https://doi.org/10.1016/j.amc.2014.04.023>
- [13] Haq, F., Islam, S., Tirmizi, I.A., A numerical technique for solution of the MRLW equation using quartic B-splines, *Appl. Math. Model.*, 34(2010) 4151-4160. <https://doi.org/10.1016/j.apm.2010.04.012>
- [14] Hammad, D.A., El-Azab, M.S., Chebyshev–Chebyshev spectral collocation method for solving the generalized regularized long wave (GRLW) equation, *Appl. Math. Comput.*, 285 (2016), 228–240. <https://doi.org/10.1016/j.amc.2016.03.033>
- [15] Jain, P.C., Shankar, R., Singh, T.V., Numerical solution of regularized long-wave equation, *Commun. Numer. Methods Eng.*, 9(1993), 579-586. <https://doi.org/10.1002/cnm.1640090705>

- [16] Karakoc, S.B.G., Uçar, Y., Yağmurlu, N.M., Numerical solutions of the MRLW equation by cubic B-spline Galerkin finite element method, *Kuwait J. Sci.*, 42 (2) (2015) 141-159.
- [17] Khalifa, A.K., Raslan, K.R., Alzubaidi, H.M., A finite difference scheme for the MRLW and solitary wave interactions, *Appl. Math. Comput.*, 189 (2007) 346-354. <https://doi.org/10.1016/j.amc.2006.11.104>
- [18] Karakoc, S.B.G., Geyikli, T., Petrov-Galerkin finite element method for solving the MRLW equation, *Math. Sci.*, 7(25) (2013). <https://doi.org/10.1186/2251-7456-7-25>
- [19] Karakoc, S.B.G., Geyikli, T., Bashan, A., A numerical solution of the modified regularized long wave (MRLW) equation using quartic B-splines, *TWMS J. Appl. Eng. Math.*, 3 (231) (2013)
- [20] Karakoç, S.B.G., Zeybek, H., Solitary-wave solutions of the GRLW equation using septic B-spline collocation method, *Appl. Math. Comput.*, 289 (2016) 159-171. <https://doi.org/10.1016/j.amc.2016.05.021>
- [21] Karakoc, S.B.G., Yağmurlu, N.M., Uçar, Y., Numerical approximation to a solution of the modified regularized long wave equation using quintic B-splines, *Boundary Value Problems*, 27 (2013). <https://doi.org/10.1186/1687-2770-2013-27>
- [22] Khalifaa, A.K., Raslana, K.R., Alzubaidib, H.M., A collocation method with cubic B-splines for solving the MRLW equation, *Journal of Computational and Applied Mathematics*, 212 (2008) 406 - 418. <https://doi.org/10.1016/j.cam.2006.12.029>
- [23] Kutluay, S., Esen, A., A finite difference solution of the regularized long wave equation, *Mathematical Problems in Engineering*, (2006). <https://doi.org/10.1155/MPE/2006/85743>
- [24] Mei, L., Chen, Y., Numerical solutions of RLW equation using Galerkin method with extrapolation techniques, *Comput. Phys. Commun.*, 183 (2012), 1609-1616. <https://doi.org/10.1016/j.cpc.2012.02.029>
- [25] Mei, L., Chen, Y., Explicit multistep method for the numerical solution of RLW equation, *Appl. Math. Comput.*, 218 (2012), 9547-9554. <https://doi.org/10.1016/j.amc.2012.03.050>
- [26] MacNamara, S., Strang, G., Operator Splitting. In: Glowinski R., Osher S., Yin W. (eds) *Splitting Methods in Communication, Imaging, Science, and Engineering*, Springer, 2016.
- [27] Mohammadi, M., Mokhtari, R., Solving the generalized regularized long wave equation on the basis of a reproducing kernel space, *J. Comput. Appl. Math.*, 235 (2011). 4003-4014. <https://doi.org/10.1016/j.cam.2011.02.012>
- [28] Mohammadi, R., Exponential B-spline collocation method for numerical solution of the generalized regularized long wave equation, *Chin. Phys. B*, 24 (2015), 050206. <https://doi.org/10.1088/1674-1056/24/5/050206>
- [29] Olver, P.J., Euler operators and conservation laws of the BBM equation, *Mathematical Proceedings of the Cambridge Philosophical Society*, 85 (1979), 143-159. <https://doi.org/10.1017/S0305004100055572>
- [30] Oruç, O., Bulut, F., Esen, A., Numerical solutions of regularized long wave equation by Haar wavelet method, *Mediterr. J. Math.*, 13 (2016), 3235-3253. <https://doi.org/10.1007/s00009-016-0682-z>
- [31] Prenter, P.M., *Splines and Variational Methods*, Wiley, New York, 1975.
- [32] Peregrine, D.H., Calculations of the development of an undular bore, *J. Fluid Mech.*, 25(1966), 321-330. <https://doi.org/10.1017/S0022112066001678>
- [33] Ramos, J.I., Solitary wave interactions of the GRLW equation, *Chaos Solit. Fractals*, 33 (2007), 479-491. <https://doi.org/10.1016/j.chaos.2006.01.016>
- [34] Raslan, K.R., El-Danaf, T.S., Solitary waves solutions of the MRLW equation using quintic B-splines, *J. King Saud Univ. Sci.*, 22 (2010), 161-166. <https://doi.org/10.1016/j.jksus.2010.04.004>
- [35] Raslan, K.R., A computational method for the regularized long wave (RLW) equation, *Appl. Math. Comput.*, 167 (2005), 1101-1118. <https://doi.org/10.1016/j.amc.2004.06.130>

- [36] Raslan, K.R., Numerical study of the modified regularized long wave (MRLW) equation, *Chaos Soliton Fractals*, 42 (2009), 1845–1853. <https://doi.org/10.1016/j.chaos.2009.03.098>
- [37] Roshan, T., A Petrov-Galerkin method for solving the generalized regularized long wave (GRLW) equation, *Comput. Math. Appl.*, 63 (2012), 943–956. <https://doi.org/10.1016/j.camwa.2011.11.059>
- [38] Saumya Ranjan Jena, S.R., Senapati, A., Gebremedhin, G.S., Approximate solution of MRLW equation in B-spline environment, *Math. Sci.*, 14 (2020), 345–357. <https://doi.org/10.1007/s40096-020-00345-6>
- [39] Soliman, A.A., Hussien, M.H., Collocation solution for RLW equation with septic spline, *Appl. Math. Comput.* 161 (2005), 623–636. <https://doi.org/10.1016/j.amc.2003.12.053>
- [40] Soliman, A.A., Raslan, K.R., Collocation method using quadratic B-spline for the RLW equation, *Int. J. Comput. Math.*, 78 (2001), 399–412. <https://doi.org/10.1080/00207160108805119>
- [41] Saka, B., Dag, I., Dogan, A., Galerkin method for the numerical solution of the RLW equation using quadratic B-splines, *Int. J. Comput. Math.*, 81(6) (2004), 727–739. <https://doi.org/10.1016/j.cam.2005.04.026>
- [42] Trotter, H. F., On the product of semi-groups of operators, *Proc. American Math. Society*, 10 (1959) 545–551.
- [43] Xiao, X., Gui, D., Feng, X., A highly efficient operator-splitting finite element method for 2D/3D nonlinear Allen–Cahn equation, *International Journal of Numerical Methods for Heat and Fluid Flow*, 27 (2017), 530–542. <https://doi.org/10.1108/HFF-12-2015-0521>
- [44] Yagmurlu, N.M., Ucar, Y., Celikkaya, İ., Operator splitting for numerical solutions of the RLW equation, *Journal of Applied Analysis and Computation*, 8(5) 2018, 1494–1510. <http://jaac-online.com/DOI:10.11948/2018>
- [45] Zaki, S.I., Solitary waves of the splitted RLW equation, *Comput. Phys. Commun.*, 138 (2001), 80–91. [https://doi.org/10.1016/S0010-4655\(01\)00200-4](https://doi.org/10.1016/S0010-4655(01)00200-4)
- [46] Zeybek, H., Karakoç, S.B.G., A numerical investigation of the GRLW equation using lumped Galerkin approach with cubic B-spline, *Springer Plus*, 5(199) (2016). <https://doi.org/10.1186/s40064-016-1773-9>
- [47] Zeybek, H., Karakoç, S.B.G., A collocation algorithm based on quintic B-splines for the solitary wave simulation of the GRLW equation, *Scientia Iranica B*, 26(6) (2019), 3356–3368. <https://doi.org/10.24200/SCI.2018.20781>